associated with HSH result from defective intestinal magnesium absorption and increased renal magnesium clearance, which lead to secondary hypocalcemia due to insufficient secretion and resistance to parathyroid hormone (PTH) [2,3]. To help prevent the negative outcomes of PTH deficiency, which include severe neurological damage and even death, HSH patients require life-long oral magnesium supplementation [4,5]. In 2002, an association was identified between HSH and mutations in the gene encoding the transient receptor potential channel melastatin 6 (TRPM6), which is involved in transepithelial magnesium transport and belongs to the transient receptor potential (TRP) family of cation channels [6,7]. To date, at least 38 *TPRM6* mutations have been reported and include stop codon, frame-shift, and splice-site mutations, and exon deletions [4]. Although an apparent association exists between the development of HSH and *TRPM6* abnormality, no definitive genotype–phenotype correlation has been established between TRPM6 gene mutations and disease severity [5].

2. Patient

The patient was an infant female born as the first child of consanguineous parents of Japanese origin. The patient's family pedigree is presented in Fig. 1A. The patient was delivered without problems and had a birth weight of 2795 g. At 72 days of age, the patient had a generalized tonic seizure with apnea, and was then admitted to a local hospital. Blood examination showed hypocalcemia (1.98 mmol/l; reference value: 2.2–2.7 mmol/l); however, the symptoms improved without any specific treatment after 1 week.

At 81 days of age, the patient was referred to our hospital because of recurrent seizure. On admission, the patient presented with seizure, muscle hypotonia, and severe irritability. Although blood examination showed hypocalcemia (1.55 mmol/l), the level of parathyroid hormone (PTH) was normal (17 pg/ml, reference value: 12–92 pg/ml). Blood urea nitrogen, creatinine, electrolytes, blood glucose and urinalysis were within normal ranges. Electroencephalogram and magnetic resonance imaging of the brain did not show any specific findings. Midazolam (0.2 mg/kg/h) for seizure and calcium gluconate (calcium; 35.2 mg/kg/day) for hypocalcemia were administered. After admission to our hospital, hypomagnesemia was detected (0.10 mmol/l; reference value: 0.75–1.25 mmol/l). Fractional magnesium excretion ($FEMg^{+2}$) was 2.7% (reference value: 1.0–8.0%), indicating that the renal absorption of magnesium was impaired. For this reason, magnesium was intravenously administered (4.37–5.47 mg/kg/day) at 84 days of age. All symptoms disappeared in accordance with normalization of the serum magnesium level. Creatinine clearance and urinary electrolytes, including calcium excretion, were within normal ranges. Renal ultrasonography was normal. Based on these findings, the patient was clinically diagnosed with HSH.

At 93 days of age, the patient was orally administered magnesium (26.73 mg/kg/day) four times daily in place of intravenous magnesium treatment. After 2 days of oral magnesium, the patient had mild diarrhea and irritability due to hypomagnesemia (0.49 mmol/l). The patient's irritability was reduced by increasing the dose of oral magnesium to 53.46 mg/kg/day, and the mild diarrhea also improved following the administration of oral magnesium with probiotics six times daily. The

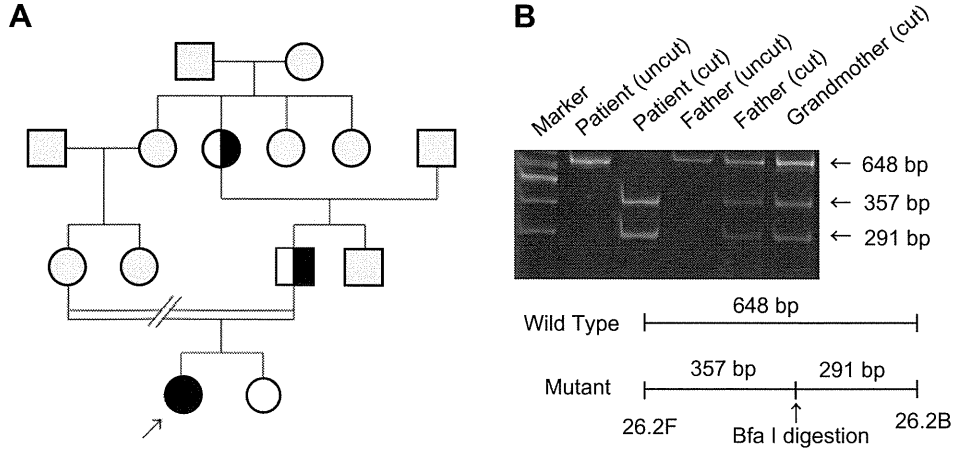

Fig. 1. Patient's family pedigree and genetic analysis of the TRPM6 gene. (A) Patient's family tree. The parents and sister of the proband did not have symptoms of HSH. Filled symbols, study patient; open symbols, wild-type haplotype; semi-filled symbols, heterozygous mutation carriers; grey symbols, unknown genotype; female; square, male; double slash, divorce. (B) Identification of the W1397X mutation in the TRPM6 gene. PCR-RFLP analysis was performed to identify mutations in the patient's TRPM6 gene using SDS–PAGE separated on an 0.8% gel. The patient has a homozygous W1397X mutation in the TRPM6 gene, and the patient's father and grandfather are heterozygous for this mutation. The restriction enzyme *Bfa*I was used in the analysis.

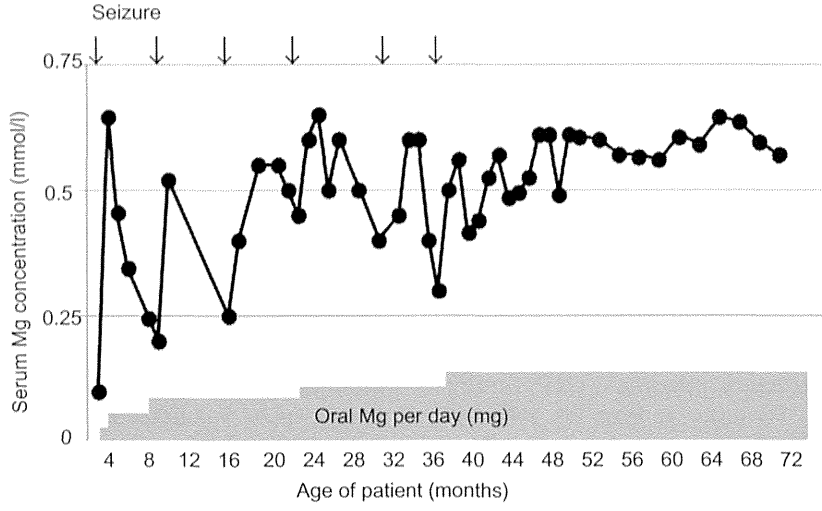

Fig. 2. Patient's clinical course. With increasing oral magnesium (Mg) administration over time, the patient's serum Mg concentration reached or exceeded the lower normal limit (0.75–1.25 mmol/l) and the number and frequency of seizures gradually decreased. Arrows indicate the occurrence of a seizure. Gray bars indicate the dose (mg/day) of orally administered Mg. The patient received a Mg dose of 101.45 mg/day at 3 months of age; 202.91 mg/day between 4 and 8 months of age; 242.40 mg/day between 8 and 24 months of age; and a maximum dose of 568.62 mg/day from 24 to 38 months of age.

patient was discharged after her serum magnesium level became stable (0.53–0.74 mmol/l) at 120 days of age. The patient's clinical course is shown in Fig. 2.

Due to poor drug compliance, the patient experienced several symptoms, including seizure, irritability, and photophobia, related to low magnesium serum levels and occasionally required intravenous infusion of magnesium until 3 years of age. The patient experienced mild diarrhea as a side effect of oral magnesium. The last reported seizure occurred at 3 years of age (Fig. 2). At 4 years of age, the patient scored 52 on an intelligence quotient test (Tanaka-Binet test) (normal > 85) and had a height of 93.0 cm (−2.7 SD for the standard height of Japanese girls). The patient was evaluated for growth hormone (GH) deficiency at 4 years and 8 months of age by performing an arginine infusion text. The patient's peak plasma GH concentration increased from 2.3 to 17.7 ng/ml after arginine infusion, suggesting that GH deficiency was not a factor.

The patient's parents provided written informed consent for the genetic analysis to be performed and for the patient's clinical data to be published. The study protocol was approved by the Ethics Committee of the Kurume University Graduate School of Medicine.

3. Methods

3.1. Mutational analysis

Extraction of DNA from white blood cells was performed using standard protocols. We designed 41 primer sets (primer sequences are available upon request) based on the sequence of the human TRPM6 gene (genomic contig GenBank accession No. NC_000009) to amplify the complete coding sequence (exons 1–39; exon 26 required 3 primer sets to cover the entire exon) and intron/exon boundaries of the TRPM6 gene from genomic DNA. Both strands of the amplified products were directly sequenced using a CEQ Dye Terminating Cycle Sequencing Kit (Beckman Coulter, Inc., Fullerton, CA) on a CEQ™ 8000 Genetic Analysis System (Beckman Coulter, Inc.). The sequences were assembled into a contig using the DNASIS Pro program (Hitachi Software Engineering Co., Ltd., Japan), and the resulting contig was aligned to the sequence of the human TRPM6 gene. To determine if the W1397X mutation was present in the patient's family members, PCR-RFLP analysis was performed using the primer set TRPP6.26.2F and TRPM6.26.2B, and the restriction endonuclease *Bfa*I.

3.2. Statistical analysis

Linear regression analysis was performed to investigate the association between the location of mutations in the TRPM6 gene and four clinical indicators of HSH: age of disease onset, initial serum magnesium and calcium concentrations (mmol/l), and dose of oral magnesium supplement (mg/kg/day) for 29 patients reported in the literature (Table 1). Patients with mutations in introns were excluded from the analysis. A total of 30 patients, which included the present study patient, were included in the analysis (Table 1) [5,6,8–12]. The level of statistical significance was set at $p > 0.05$. All analyses were performed using SPSS statistical software (SPSS Inc., Chicago, IL).

Table 1
Clinical data and *TRPM6* mutations of the 30 HSH patients analyzed in the present study.

Case	Exon	*TRPM6* mutation	Onset age (day)	Initial serum Mg/Ca (mmol/l)	Amount of oral Mg (mg/kg/day)	Refs.
1	25	Q1186X	90	0.16/1.8	4.86	[10]
2	25	Q1186X	90	0.08/1.8	9.72	[10]
3	12	R474X	16	0.32/1.78	250	[9]
4	5	E157X	35	0.16/1.43	20	[11]
5	16	S590X	60	0.21/1.63	25.03	[5,6]
6	4	S141L	120	0.1/2.50	32.81	[5,6]
7	11/26	H427fsX429 + 1260fsX283	35	0.41/1.88	75.35	[5,6]
8	17	R736fsX737	35	0.17/1.5	19.44	[5,8]
9	17	R736fsX737	35	0.22/1.6	18.23	[5,8]
10	32/33	Del exons 31 + 32	150	0.15/1.94	11.91	[5]
11	32/33	Del exons 31 + 32	35	0.22/1.73	10.21	[5]
12	22/23	Del exons 23 + 24	90	ND/1.74	9.97	[5]
13	30	L1673fsX1675	60	0.2/1.31	13.61	[5]
14	21	I944fsX959	42	ND/	13.37	[5]
15	26	Fs + preterm stp	60	0.1/1.66	72.92	[5]
16	26	Fs + preterm stp	120	0.19/	94.79	[5]
17	36	Loss of splice site/exon skipping	9	0.09/1.6	13.12	[5]
18	36	Loss of splice site/exon skipping	120	0.16/1.75	22.85	[5]
19	21	R928X	21	0.2/1.35	24.79	[5]
20	16	P599fsX609	35	0.29/1.45	42.05	[5]
21	21	Del exon 21	28	0.44/1.7	60.03	[5]
22	5	E157X	90	0.1/1.45	48.61	[5]
23	26	R1533X	60	/	17.26	[5]
24	6	D223fsX263	180	0.3/1.75		[5]
25	23	Y1053C		0.05/1.78	23.51	[12]
26	5/34	E157X + S1754 N	120	0.2/1.6	12.15	[12]
27	17	L708P + Loss of splice site	42	0.12/1.6	45.2	[12]
28	19/29	E872G + Q1663R	270	0.1/1.47	36.45	[12]
29	25	L1143P + Loss of splice site	60	0.08/1.94	18.23	[12]
30	26	W1397X	72	0.1/1.98	53.46	Present
Median	21.75		60.0	0.16/1.70	22.85	
Range	4–36		16–270	0.05–0.44/1.31–2.50	4.86–250	
p Value (vs. exon)			0.65	0.29/0.82	0.15	

Mg, magnesium; Ca, calcium; ND, not detectable; Del, deletion; Fs, frame shift.

4. Results

4.1. Mutational analysis

A novel homozygous stop-codon mutation, [c.4190 G > A] W1397X, was detected in exon 26 of the patient's TRPM6 gene based on the results of PCR-RFLP analysis (Fig. 1B). The patient's father and paternal grandmother were heterozygous for this mutation, whereas the patient's younger sister had wild-type *TRPM6* alleles (Fig. 1A). No member of the patient's immediate family had any clinical symptoms of HSH or abnormal laboratory findings related to serum magnesium, calcium, phosphate, and intact PTH levels. Unfortunately, the genotype of the patient's mother could not be determined as she was separated from the family due to divorce. Based on the genotype of the patient and the patient's father, the mother was likely heterozygous for the W1397X mutation. However, because no molecular analyses for chromosomal abnormalities were performed, we cannot exclude the possibility of uniparental disomy from the patient's father.

4.2. Association between TRPM6 gene mutation location and clinical data of HSH

To investigate if a correlation exists between the degree of loss of function of the TRPM6 protein

resulting from gene mutation and HSH severity we retrospectively analyzed the reported clinical data of 30 HSH patients, including the present study patient, with mutations in exons of the TRPM6 gene (Table 1). Linear regression analysis was performed for several clinical parameters of HSH, specifically disease onset age, initial serum magnesium and calcium concentrations, and oral magnesium dose. However, no significant correlations between the total number of exons in the TRPM6 gene and each of the four examined parameters of HSH severity were detected.

5. Discussion

We identified the first Japanese HSH patient with a novel homozygous stop-codon mutation in exon 26 of the TRPM6 gene. The patient manifested recurrent seizures at 10 weeks of age, leading to the diagnosis of HSH, and suffered from both physical and mental impairment in the form of short stature and mental retardation despite magnesium supplementation. One of the underlying causes of the complications was possibly due to poor drug compliance as a result of family problems. The retrospective analysis of 29 HSH patients with TRPM6 gene mutations did not detect a relationship between mutation location and any of the four indicators of HSH. Our findings suggest that preventing severe complications of HSH requires early diagnosis and good drug compliance to avoid recurrent seizures and permanent mental damage. In addition, clinical data for serum calcium and magnesium levels is not expected to aid in the genetic screening of nonsense mutations in the TRPM6 gene.

Our HSH patient exhibited early signs of mild mental retardation and had a low IQ test score at 4 years of age. Although HSH patients typically have normal psychomotor development, delayed diagnosis and repeated convulsions can cause mild to severe mental retardation as a result of neurological damage [4,5]. In the present patient, mental retardation may have resulted from the slightly delayed diagnosis of HSH and unstable serum magnesium levels associated with frequent diarrhea, which resulted in repeated convulsions over a 2.5-years period. In addition, family problems led to inadequate nurturing and low drug compliance, which likely contributed to the patient's low serum magnesium levels, convulsions, and mental impairment.

The patient's symptoms, particularly the frequency of seizures, gradually improved with increasing serum magnesium levels. Several additional factors may have influenced the patient's clinical improvement, including the oral administration of probiotics, avoidance of allergic foods, and improved family care. Although the mechanisms by which hypomagnesemia causes neurological damage are unknown, impaired voltage-dependent magnesium gating of the N-methyl-D-aspartate receptor may induce seizures [13,14]. In TRPM6 knockout mice, abnormal development and neural tube defects were observed [15], suggesting that TRPM6 affects nerve development. Mental retardation has also been reported in HSH patients due to the delayed administration of magnesium [4,5]. Our patient experienced seizures when serum magnesium fell below 0.4 mmol/l as a result of poor drug compliance. Thus, the rapid diagnosis of HSH and supplementation of magnesium above a threshold serum level are important to prevent psychomotor impairment.

Our patient had short stature and failed to thrive. Although growth disorders are rarely observed in HSH patients and the underlying mechanisms remain unclear [5,14], inadequate nutrition might be a major contributing factor. It is also possible that our patient's unstable family environment impacted her development, as short stature and failure to thrive have been reported for children who have suffered from physical and mental abuse [16–19]. At the time of writing, the patient had stable serum magnesium levels, was free from family problems, and had normal GH secretion. Thus, it is possible that young HSH patients with short stature and failure to thrive may improve with continued magnesium supplementation.

Schlingmann et al. [5] first reported that no genotype–phenotype correlation exists for HSH, and since this publication, a definitive genotype–phenotype correlation has not been demonstrated for this disorder. Most of the mutations in the HSH patients included in the present analyses (Table 1) would theoretically result in nonsense-mediated decay of TRPM6 mRNA and caused reduced TRPM6 protein translation [20]. Moreover, due to the large size of the TRPM6 gene, which consists of 39 exons spanning 167 kb of genomic sequence and codes for a protein of 2022 amino acids (Fig. 3), mutational screening is time consuming and expensive. If nonsense mutations leading to protein dysfunction or rapid mRNA decay could be predicted from clinical data, it would increase the efficiency of mutational screening and detection. We speculated that the total number of exons encoding the protein may be correlated with the clinical parameters of HSH. However, our present analyses of 30 HSH patients suggest that no correlation exists between TRPM6 genotype and the clinical parameters of HSH, demonstrating that clinical data are not useful for the estimation of the exon mutation site.

Several limitations of the present study warrant mention. First, as only one HSH patient with a stop-codon mutation in exon 26 of the TRPM6 gene was analyzed, our findings need to be confirmed in other patients who also possessed the identified mutation. Second, the linear regression analysis only included the data of 30 patients, a sample size that may have been too small to

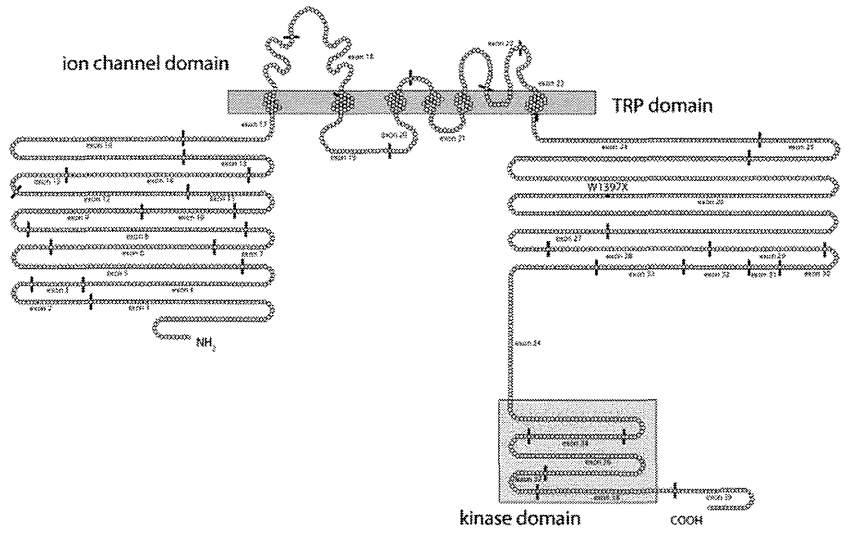

Fig. 3. Structure of the TRPM6 gene and exons. The TRPM6 gene consists of 39 exons spanning 167 kb of genomic sequence and coding for a protein of 2022 amino acids. The TRPM6 protein harbors an ion channel region with six transmembrane domains and a putative pore region between the fifth and sixth transmembrane domain, a long N-terminus conserved within the TRPM family, a TRP domain of unknown function located C-terminally of the ion channel domain, and a C-terminal kinase domain with sequence similarity to atypical α kinases. The structural organization of the TRPM6 gene presented in this figure was adapted from Ref. [20].

detect a relationship between exon number of the genetic abnormality and serum magnesium levels. Finally, the trend of increasing magnesium levels with the increasing level of TRPM6 gene impairment may have been influenced by differences in the therapeutic strategies between patients.

6. Conclusions

We describe here a Japanese HSH patient with a novel mutation in exon 26 of the TRPM6 gene. Despite the administration of magnesium at 12 weeks of age, the patient experienced family problems that may have adversely affected drug compliance, leading to short stature and mental retardation. The location analysis of mutations in the protein-coding region (exon number) of TRPM6 in 30 HSH patients and the 4 examined clinical parameters of disease showed that no genotype–phenotype correlation exists for HSH, as has been reported previously.

Acknowledgement

This work was supported in part by a grant (#16390308) from the Ministry of Culture and Education in Japan to Y.K.

Appendix A. Supplementary data

Supplementary data associated with this article can be found, in the online version, at http://dx.doi.org/10.1016/j.braindev.2014.06.006.

References

[1] Paunier L, Raddle IC, Kooh SW, Conen PE, Fraser D. Primary hypomagnesemia with secondary hypocalcemia in an infant. Pediatrics 1968;41:385–402.
[2] Lombeck I, Ritzl F, Schnippering HG, Michael H, Bremer HJ, Feinendegen LE, et al. Primary hypomagnesemia. I. Absorption Studies. Z Kinderheilkd 1975;118:249–58.
[3] Milla PJ, Aggett PJ, Wolff OH, Harries JT. Studies in primary hypomagnesaemia: evidence for defective carrier-mediated small intestinal transport of magnesium. Gut 1979;20:1028–33.
[4] Shalev H, Phillip M, Galil A, Carmi R, Landau D. Clinical presentation and outcome in primary familial hypomagnesaemia. Arch Dis Child 1998;78:127–30.
[5] Schlingmann KP, Sassen MC, Weber S, Pechmann U, Kusch K, Pelken L, et al. Novel TRPM6 mutations in 21 families with primary hypomagnesemia and secondary hypocalcemia. J Am Soc Nephrol 2005;16:3061–9.
[6] Schlingmann KP, Weber S, Peters M, Niemann Nejsum L, Vitzthum H, Klingel K, et al. Hypomagnesemia with secondary hypocalcemia is caused by mutations in TRPM6, a new member of the TRPM gene family. Nat Genet 2002;31:166–70.
[7] Walder RY, Landau D, Meyer P, Shalev H, Tsolia M, Borochowitz Z, et al. Mutation of TRPM6 causes familial hypomagnesemia with secondary hypocalcemia. Nat Genet 2002;31:171–4.
[8] Challa A, Papaefstathiou I, Lapatsanis D, Tsolas O. Primary idiopathic hypomagnesemia in two female siblings. Acta Paediatr 1995;84:1075–8.
[9] Esteban-Oliva D, Pintos-Morell G, Konrad M. Long-term follow-up of a patient with primary hypomagnesaemia and secondary hypocalcaemia due to a novel TRPM6 mutation. Eur J Pediatr 2009;168:439–42.
[10] Guran T, Akcay T, Bereket A, Atay Z, Turan S, Haisch L, et al. Clinical and molecular characterization of Turkish patients with familial hypomagnesaemia: novel mutations in TRPM6 and CLDN16 genes. Nephrol Dial Transplant 2012;27:667–73.
[11] Apa H, Kayserili E, Agin H, Hizarcioglu M, Gulez P, Berdeli A. A case of hypomagnesemia with secondary hypocalcemia caused by Trpm6 gene mutation. Indian J Pediatr 2008;75:632–4.

[12] Lainez S, Schlingmann KP, van der Wijst J, Dworniczak B, van Zeeland F, Konrad M, et al. New TRPM6 missense mutations linked to hypomagnesemia with secondary hypocalcemia. Eur J Hum Genet 2013;1–8.
[13] Mody I, Lambert JD, Heinemann U. Low extracellular magnesium induces epileptiform activity and spreading depression in rat hippocampal slices. J Neurophysiol 1987;57:869–88.
[14] Hartnett KA, Stout AK, Rajdev S, Rosenberg PA, Reynolds IJ, Aizenman E. NMDA receptor-mediated neurotoxicity: a paradoxical requirement for extracellular Mg^{2+} in Na^{+}/Ca^{2+}-free solutions in rat cortical neurons in vitro. J Neurochem 1997;68:1836–45.
[15] Walder RY, Yang B, Stokes JB, Kirby PA, Cao X, Shi P, et al. Mice defective in Trpm6 show embryonic mortality and neural tube defects. Hum Mol Genet 2009;18:4367–75.
[16] Cole DE, Kooh SW, Vieth R. Primary infantile hypomagnesaemia: outcome after 21 years and treatment with continuous nocturnal nasogastric magnesium infusion. Eur J Pediatr 2000;159:38–43.
[17] Munoz-Hoyos A, Molina-Carballo A, Augustin-Morales M, Contreras-Chova F, Naranjo-Gomez A, Justicia-Martinex F, et al. Psychosocial dwarfism: psychopathological aspects and putative neuroendocrine markers. Psychiatry Res 2011;188:96–101.
[18] Japtap VS, Sarathi V, Lila AR, Bukan AP, Bandgar T, Menon P, et al. Hyperphagic short stature: a case report and review of literature. Indian J Endocrinol Metab 2012;16:624–6.
[19] Skuse D, Albanese A, Stanhope R, Gilmour J, Voss L. A new stress-related syndrome of growth failure and hyperphagia in children associated with reversibility of growth-hormone insufficiency. Lancet 1996;348:353–8.
[20] Schlingmann KP, Waldegger S, Konrad M, Chubanov V, Gudermann T. TRPM6 and TRPM7—Gatekeepers of human magnesium metabolism. Biochim Biophys Acta 2007;1772:813–21.

AUTHOR QUERY FORM

Journal: CMET

Article Number: 1726

Dear Author,

Please check your proof carefully and mark all corrections at the appropriate place in the proof.

Location in article	Query / Remark: Click on the Q link to find the query's location in text Please insert your reply or correction at the corresponding line in the proof
	There are no queries in this article

Thank you for your assistance.

Article

Cell Metabolism

Cdk5rap1-Mediated 2-Methylthio Modification of Mitochondrial tRNAs Governs Protein Translation and Contributes to Myopathy in Mice and Humans

Graphical Abstract

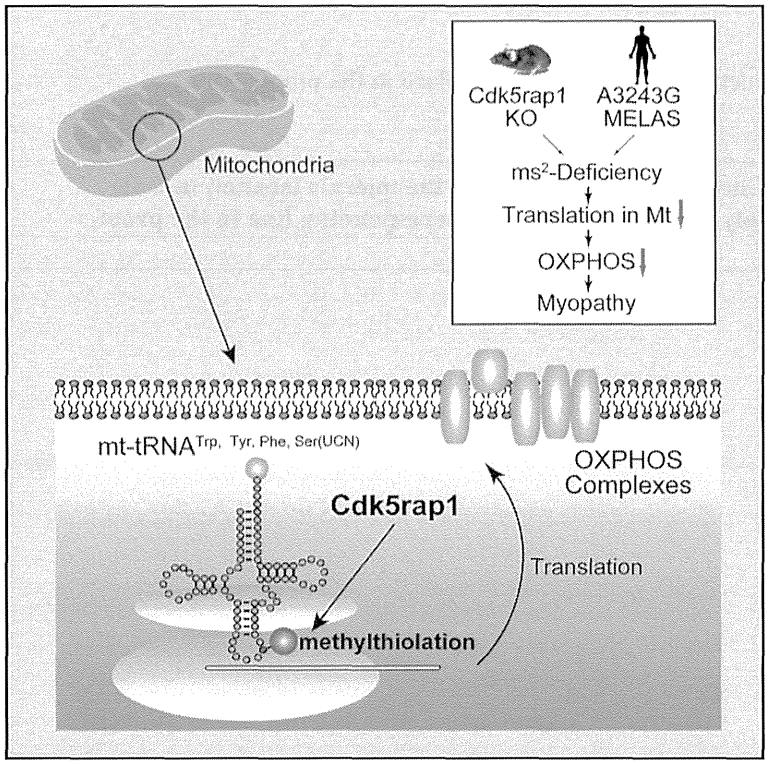

Authors

Fan-Yan Wei, Bo Zhou, ..., Yuichi Oike, Kazuhito Tomizawa

Correspondence

tomikt@kumamoto-u.ac.jp

In Brief

Wei et al. report that Cdk5rap1 is responsible for 2-methylthio (ms^2) modifications of mammalian mt-tRNAs. The modification is critical for efficient mitochondrial translation in mice and dysregulated in MELAS patients.

Highlights

- Cdk5rap1 catalyzes 2-methylthio (ms^2) modification of four mitochondrial tRNAs
- The ms^2 modifications optimize mitochondrial translation and OXPHOS activity
- Deficiency of ms^2 modification accelerates myopathy and cardiac dysfunction in mice
- The ms^2 modification levels are reduced in patients with mitochondrial disease

Wei et al., 2015, Cell Metabolism *21*, 1–15
March 3, 2015 ©2015 Elsevier Inc.
http://dx.doi.org/10.1016/j.cmet.2015.01.019

Please cite this article in press as: Wei et al., Cdk5rap1-Mediated 2-Methylthio Modification of Mitochondrial tRNAs Governs Protein Translation and Contributes to Myopathy in Mice and Humans, Cell Metabolism (2015), http://dx.doi.org/10.1016/j.cmet.2015.01.019

Cell Metabolism
Article

CellPress

Cdk5rap1-Mediated 2-Methylthio Modification of Mitochondrial tRNAs Governs Protein Translation and Contributes to Myopathy in Mice and Humans

Fan-Yan Wei,[1,7] Bo Zhou,[1,7] Takeo Suzuki,[3] Keishi Miyata,[2] Yoshihiro Ujihara,[4] Haruki Horiguchi,[2] Nozomu Takahashi,[1] Peiyu Xie,[1] Hiroyuki Michiue,[5] Atsushi Fujimura,[5] Taku Kaitsuka,[1] Hideki Matsui,[5] Yasutoshi Koga,[6] Satoshi Mohri,[4] Tsutomu Suzuki,[3] Yuichi Oike,[2] and Kazuhito Tomizawa[1,*]

[1]Department of Molecular Physiology
[2]Department of Molecular Genetics
Faculty of Life Sciences, Kumamoto University, Kumamoto 860-8556, Japan
[3]Department of Chemistry and Biotechnology, School of Engineering, The University of Tokyo, Tokyo 113-8656, Japan
[4]First Department of Physiology, Kawasaki Medical School, Okayama 701-0192, Japan
[5]Department of Physiology, Okayama University Graduate School of Medicine, Dentistry and Pharmaceutical Sciences, Okayama 700-8558, Japan
[6]Department of Pediatrics and Child Health, Kurume University Graduate School of Medicine, Fukuoka 830-0011, Japan
[7]Co-first author
*Correspondence: tomikt@kumamoto-u.ac.jp
http://dx.doi.org/10.1016/j.cmet.2015.01.019

SUMMARY

Transfer RNAs (tRNAs) contain a wide variety of post-transcriptional modifications that are important for accurate decoding. Mammalian mitochondrial tRNAs (mt-tRNAs) are modified by nuclear-encoded tRNA-modifying enzymes; however, the physiological roles of these modifications remain largely unknown. In this study, we report that Cdk5 regulatory subunit-associated protein 1 (Cdk5rap1) is responsible for 2-methylthio (ms^2) modifications of mammalian mt-tRNAs for Ser(UCN), Phe, Tyr, and Trp codons. Deficiency in ms^2 modification markedly impaired mitochondrial protein synthesis, which resulted in respiratory defects in Cdk5rap1 knockout (KO) mice. The KO mice were highly susceptive to stress-induced mitochondrial remodeling and exhibited accelerated myopathy and cardiac dysfunction under stressed conditions. Furthermore, we demonstrate that the ms^2 modifications of mt-tRNAs were sensitive to oxidative stress and were reduced in patients with mitochondrial disease. These findings highlight the fundamental role of ms^2 modifications of mt-tRNAs in mitochondrial protein synthesis and their pathological consequences in mitochondrial disease.

INTRODUCTION

Transfer RNA (tRNA) is a key molecule in the translational apparatus to decode genetic information into proteins. A unique feature of tRNAs is the presence of a variety of chemical modifications of their nucleotides (Machnicka et al., 2013). These modifications are critical for efficient and accurate decoding (Agris, 2004; Suzuki, 2005). To date, more than 100 modified nucleotides have been identified in tRNAs from the three domains of life, indicative of the universal importance of tRNA modifications (Machnicka et al., 2013).

Given the critical roles of tRNA modifications in cells, it is not surprising that tRNA modification deficiencies have been associated with human diseases (Torres et al., 2014). Genetic variations in the gene encoding Cdk5 regulatory subunit associated protein 1-like-1 (CDKAL1), which inserts a 2-methylthio (ms^2) group into the N^6-threonylcarbamoyl adenosine (t^6A) of cytosolic $tRNA^{Lys}(UUU)$, have been associated with the development of type 2 diabetes (Steinthorsdottir et al., 2007; Arragain et al., 2010). A deficiency in the ms^2 modification of $tRNA^{Lys}(UUU)$ resulted in aberrant proinsulin synthesis, which ultimately led to impaired glucose metabolism and insulin secretion in Cdkal1 knockout (KO) mice and in human subjects carrying T2D-associated alleles of *CDKAL1* (Wei et al., 2011; Xie et al., 2013).

In mitochondrial tRNAs (mt-tRNAs), 15 species of modified nucleotides at 118 positions have been identified in bovine (Suzuki and Suzuki, 2014). Some of these modifications have been associated with the development of mitochondrial diseases, such as Mitochondrial myopathy, encephalopathy, lactic cidosis, stroke-like episodes (MELAS), and myoclonus epilepsy with ragged-red fibers (MERRF) (Suzuki et al., 2011). mt-$tRNA^{Leu}$ and mt-$tRNA^{Lys}$ contain 5-taurinomethyl (τm^5) and 5-taurinomethyl-2-thio ($\tau m^5 s^2$) modifications, respectively, at U34 (Yasukawa et al., 2001; Suzuki et al., 2002), and both of these modifications are critical for decoding their cognate codons (Kirino et al., 2004; Yasukawa et al., 2001). The absence of these modifications has been observed in MELAS patients carrying the A3243G mutation in mt-$tRNA^{Leu}$ and in MERRF patients carrying the A8344G mutation in mt-$tRNA^{Lys}$ (Yasukawa et al., 2001). These results suggest a critical role for mt-tRNA modifications in the pathogenesis of human diseases. Nevertheless, knowledge regarding the physiological roles of tRNA modifications is incomplete, and a complete investigation of the individual types of mt-tRNA modifications is required to fully understand the physiological function and molecular pathology of tRNA modifications in human diseases.

In mammalian mt-tRNAs, 2-methylthio-N^6-isopentenyl adenosine (ms^2i^6A) is a unique modification that is conserved in all three domains of life (Machnicka et al., 2013). In bacteria, the ms^2 modification of ms^2i^6A contributes to accurate decoding by improving tRNA binding to codons (Urbonavicius et al., 2001; Jenner et al., 2010). However, the physiological importance of ms^2 modifications in mammals is unknown. We have previously shown that Cdk5rap1 might be responsible for the ms^2 modification of ms^2i^6A because of its homology to Cdkal1, which catalyzes ms^2t^6A modification (Arragain et al., 2010). Recently, Cdk5rap1 was proposed to catalyze ms^2 group insertion in both cytosolic RNAs and mt-tRNAs; however, the exact substrate tRNA of Cdk5rap1 in mammalian cells remains unclear (Reiter et al., 2012).

Given the exclusive mitochondrial localization of ms^2i^6A in mammals and the implication of this localization in the decoding process, we hypothesize that Cdk5rap1 might specifically catalyze the ms^2 modification of mt-tRNAs and contribute to mitochondrial function in vivo. In this study, we validated this hypothesis through a thorough investigation of the physiological function of the ms^2 modification in Cdk5rap1 KO mice. Furthermore, we investigated the pathological implication and the molecular mechanism of the ms^2 modification in MELAS patients.

RESULTS

Cdk5rap1 Catalyzes the Conversion of i^6A to ms^2i^6A in Mitochondrial tRNAs

Based on the high homology between mammalian Cdk5rap1 and bacterial MiaB, we and another group previously showed that Cdk5rap1 might be a mammalian methylthiotransferase that catalyzes the conversion of N^6-isopentenyl adenosine (i^6A) to 2-methylthio-N^6-isopentenyl adenosine (ms^2i^6A) (Figure 1A and see Figure S1A available online; Arragain et al., 2010; Reiter et al., 2012). To investigate this hypothesis, we transformed Cdk5rap1 in MiaB-deficient bacteria (ΔMiaB), which do not contain ms^2 modifications. As expected, the transformation of Cdk5rap1 restored ms^2 modifications (Figure 1B). The conserved cysteine residues in the UPF domain and the radical SAM domain of MiaB are critical for ms^2 modification through their interaction with two [4Fe-4S] clusters (Forouhar et al., 2013). Similar to MiaB, the mutation of cysteine residues in the UFP domain or the radical SAM domain of Cdk5rap1 completely abolished the ms^2 modification (Figure 1B).

To prove that Cdk5rap1 is a mitochondrial methylthiotransferase and to identify its exact substrates, we generated Cdk5rap1 KO mice (Figures S1B–S1D). As expected, the ms^2 modification was completely abolished in KO mice (Figures S1E and S1F). Cdk5rap1 colocalized with Mitotracker in HeLa cells (Figure S2A). Cdk5rap1 with a deletion of mitochondrial localization signal at the N terminus exhibited cytosolic localization but retained its enzyme activity (Figures S2A and S2B). However, no ms^2 modification was detected in Cdk5rap1-deficient mouse embryonic fibroblast (MEF) cells expressing the cytosolic form of Cdk5rap1 (Figures S2C and S2D). These results indicate that Cdk5rap1 localizes on mitochondria and specifically modifies mt-tRNAs. To identify the exact substrate of Cdk5rap1, individual mt-tRNA was isolated from WT and KO mice and subjected to mass spectrometric analysis. The ms^2 modification was completely absent at A37 in mt-$tRNA^{Phe}$, mt-$tRNA^{Trp}$, mt-$tRNA^{Tyr}$, and mt-$tRNA^{Ser(UCN)}$ isolated from KO mice (Figures 1C–1F). The absence of an ms^2 modification did not affect the nearby $_T m^5$ modification at U34 in mt-$tRNA^{Trp}$ (Figure S1F). These results clearly demonstrate that Cdk5rap1 is a two [4Fe-4S] cluster-containing mitochondrial methylthiotransferase that specifically converts i^6A to ms^2i^6A at A37 of mt-$tRNA^{Phe}$, mt-$tRNA^{Trp}$, mt-$tRNA^{Tyr}$, and mt-$tRNA^{Ser(UCN)}$ in mammalian cells.

The ms^2 Modification Controls Codon-Specific Decoding Fidelity in a Translation Rate-Dependent Manner

A previous study demonstrated that the ms^2 group of 2-methylthio-N^6-hydroxyisopentenyl adenosine (ms^2io^6A) is critical for the accurate decoding of Tyr and Phe codons (Urbonavicius et al., 2001). To thoroughly investigate the role of ms^2 modifications of tRNAs during the decoding of their cognate codons, we utilized a luciferase-based reporter and transformed the plasmid into a WT strain or the ΔMiaB strain to detect frameshifting in the presence or absence of the ms^2 modification. The firefly luciferase gene was properly translated only when frameshifting occurred at the cognate codons read by $tRNA^{Phe}$, $tRNA^{Trp}$, $tRNA^{Tyr}$, or $tRNA^{Ser(UCN)}$ (Figure S2E). A deficiency in ms^2 modification induced frameshifting at Phe(TTT) and Tyr(TAT) codons (Figure 1G). Induction of protein translation by isopropyl-beta-D-thiogalactopyranoside (IPTG) exaggerated the overall frameshifting rate in both the WT and ΔMiaB strains. In addition to the Phe(TTT) and Tyr(TAT) codons, there was a significant increase in ms^2-dependent frameshifting at the Tyr(TAC), Ser(TCT), Ser(TCC), and Ser(TCG) codons, for which frameshifting was not observed without IPTG induction (Figures S1G–S1I). Importantly, these results show that ms^2-dependent frameshifting specifically occurred during the translation of wobble codons, such as Phe(TTT), Tyr(TAT), Ser(TCT), Ser(TCC), and Ser(TCG), with the exception of the Tyr(TAC) codon, but not the cognate codons, such as Phe(TTC), Ser(TCA), and Trp(TGG) (shown in red in Figures S1F–S1I). Furthermore, the ms^2-deficiency-evoked frameshifting was fully reversed by transformation with active Cdk5rap1, but not dominant-negative Cdk5rap1 (Figure 1G). These results demonstrate that ms^2 modification is critical for the accurate decoding of wobble codons corresponding to $tRNA^{Phe}$, $tRNA^{Tyr}$, or $tRNA^{Ser(UCN)}$ in a translation rate-dependent manner.

Deficiency of the Mitochondrial ms^2 Modification Attenuates Mitochondrial Translation

To examine mitochondrial protein synthesis, WT or KO MEF cells were labeled with ^{35}S-methionine for 1 hr and subjected to pulse chase. The mitochondrial protein synthesis was substantially decreased in KO MEF cells (Figure 2A). Furthermore, MEF cells were radioactively labeled and subjected to blue native PAGE to examine the formation of respiratory complexes. The incorporation of mitochondrial proteins into complexes I, III, and IV was substantially decreased in KO MEF, whereas complex V was unaffected (Figures 2B and 2C). These results suggest that the deficiency in ms^2 modification greatly attenuated mitochondrial protein synthesis, resulting in impaired complex assembly.

The maintenance of mitochondrial OXPHOS subunits is critical for the electron transport chain, which maintains the resting

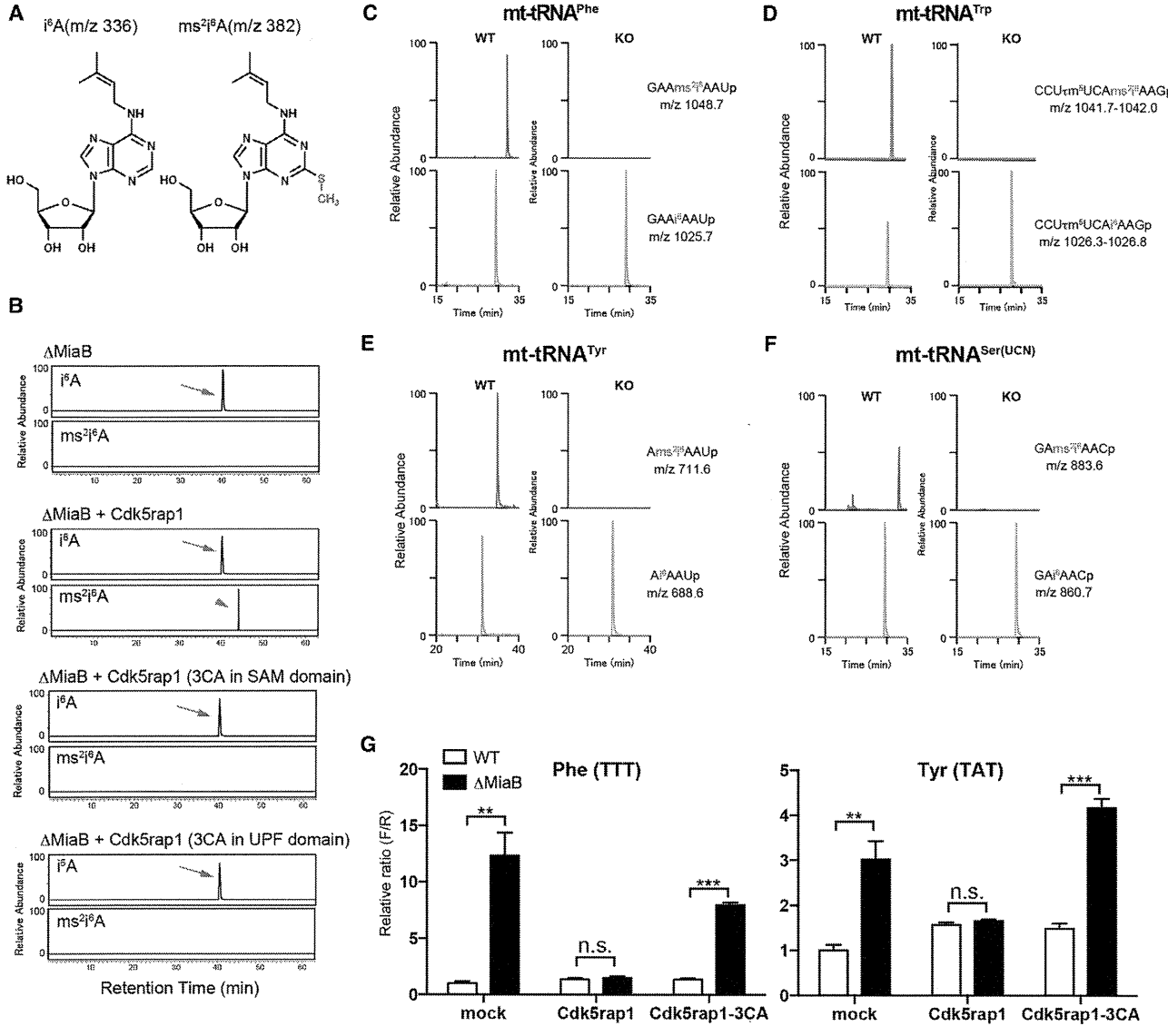

Figure 1. Cdk5rap1 Is The Mammalian mt-tRNA Methylthiotransferase

(A) Structures of N^6-isopentenyladenosine (i^6A) and 2-methylthio-N^6-isopentenyladenosine (ms^2i^6A) and the corresponding m/z values are shown. The ms^2 group ($S\text{-}CH_3$) is shown in red.

(B) GST-Cdk5rap1 or GST-Cdk5rap1 with Cys-to-Ala mutations (3CA) was transformed into the MiaB-deficient strain (ΔMiaB). The arrows and arrowhead indicate the peaks corresponding to i^6A and ms^2i^6A, respectively.

(C–F) Examination of the ms^2i^6A modification in mt-$tRNA^{Phe}$ (C), mt-$tRNA^{Trp}$ (D), mt-$tRNA^{Tyr}$ (E), and mt-$tRNA^{Ser(UCN)}$ (F) isolated from WT and KO mice by mass spectrometry. The mass chromatograms show the peaks corresponding to fragments containing i^6A or ms^2i^6A.

(G) Frameshifting assay. WT and ΔMiaB bacteria were transformed with Cdk5rap1 or inactive Cdk5rap1 (Cdk5rap1-3CA). The relative ratio of firefly luciferase activity to renilla luciferase activity (F/R) represents the decoding error. n = 4. Data are mean ± SEM. $^{**}p < 0.01$, $^{***}p < 0.0001$.

mitochondrial membrane potential and drives respiration. We thus investigated the mitochondrial membrane potential in WT and KO MEF cells. There was a marked increase in cell populations with very low membrane potential in KO MEF cells (Figure 2D). Consequently, the oxygen consumption rate in KO cells was significantly lower than that in WT MEF cells (Figure 2E). Furthermore, the KO cells quickly lost their mitochondrial membrane potential after treatment with very low doses of rotenone and FCCP, which had little effect on WT cells (Figures 2F and 2G). These results thus demonstrate that ms^2 modifications of mt-tRNAs are critical for maintaining efficient mitochondrial translation and respiratory chain.

Deficiency of Mitochondrial ms^2 Modification Impairs OXPHOS in Skeletal Muscle and Heart Tissue without Affecting Basal Metabolism

To investigate the physiological role of mitochondrial ms^2 modification, we examined the phenotype of KO mice in vivo. Despite

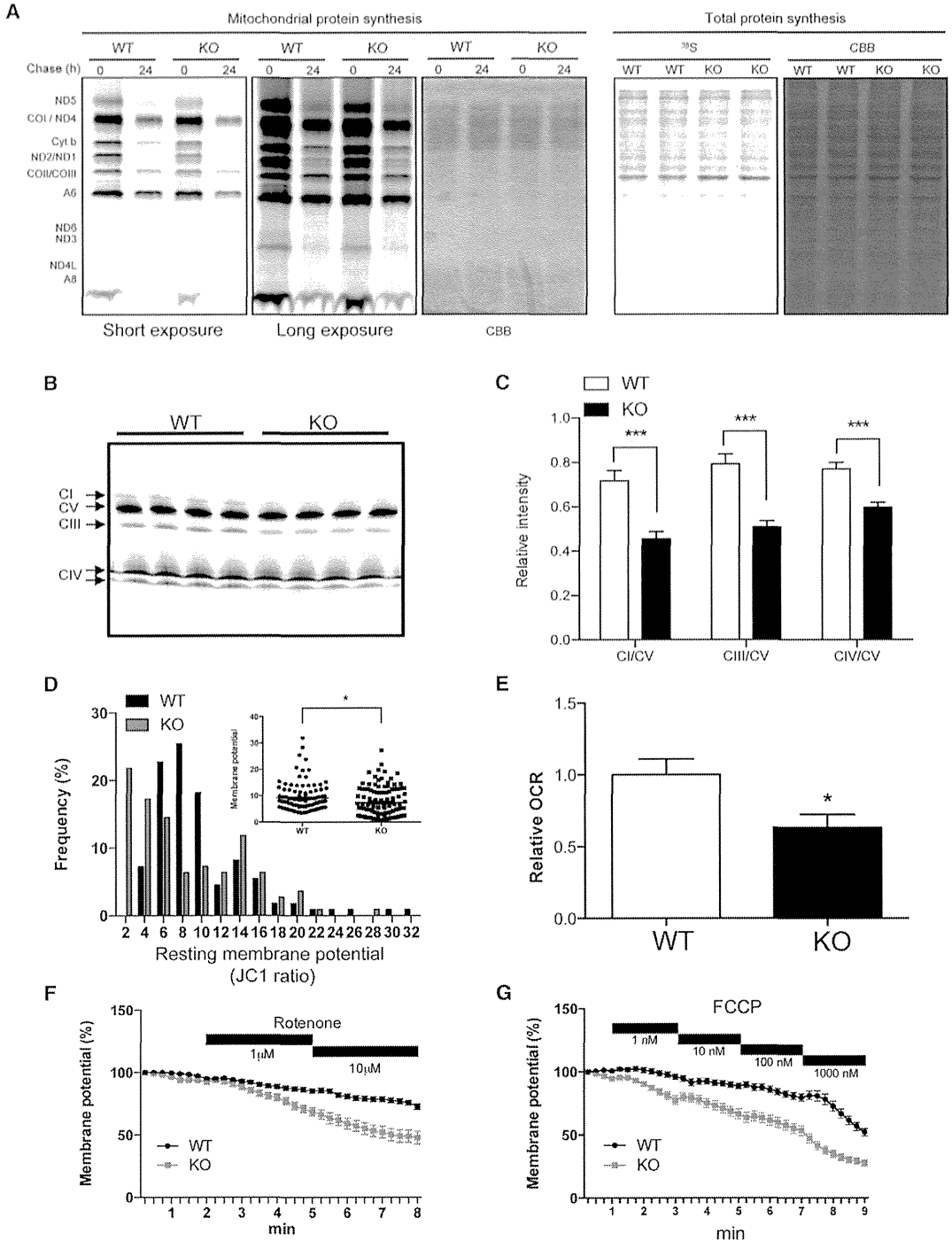

Figure 2. Deficiency in the ms^2 Modifications Impaired Mitochondrial Protein Synthesis and Mitochondrial Functions

(A) WT and KO MEF cells were labeled with ^{35}S-Met/Cys and chased for 0 or 24 hr in the presence of emetine for measurement of mitochondrial protein synthesis (left panels). MEF cells were labeled with ^{35}S-Met/Cys for 1 hr, and total protein synthesis was measured (right panels). CBB staining of gel was used as loading control.

(B and C) The autoradiogram of blue native PAGE shows a decrease in the incorporation of mitochondrial proteins in complexes I, III, and IV in KO MEF cells (B). The relative intensity of complex I, III, and IV versus complex V was quantified (C).

(D) The histogram and inserted graph show that KO MEF cells contain a number of mitochondria with low membrane potentials; n = 110 each.

(E) KO cells showed a significant decrease in the oxygen consumption rate (OCR); n = 10 each.

(E–G) Cells were stained with TMRM for measuring membrane potential. The relative membrane potential in the presence of rotenone (F) or FCCP (G) was analyzed; n = 66 for WT and n = 30 for KO (F); n = 43 for WT and n = 32 for KO (G). Data are mean ± SEM. *p < 0.05.

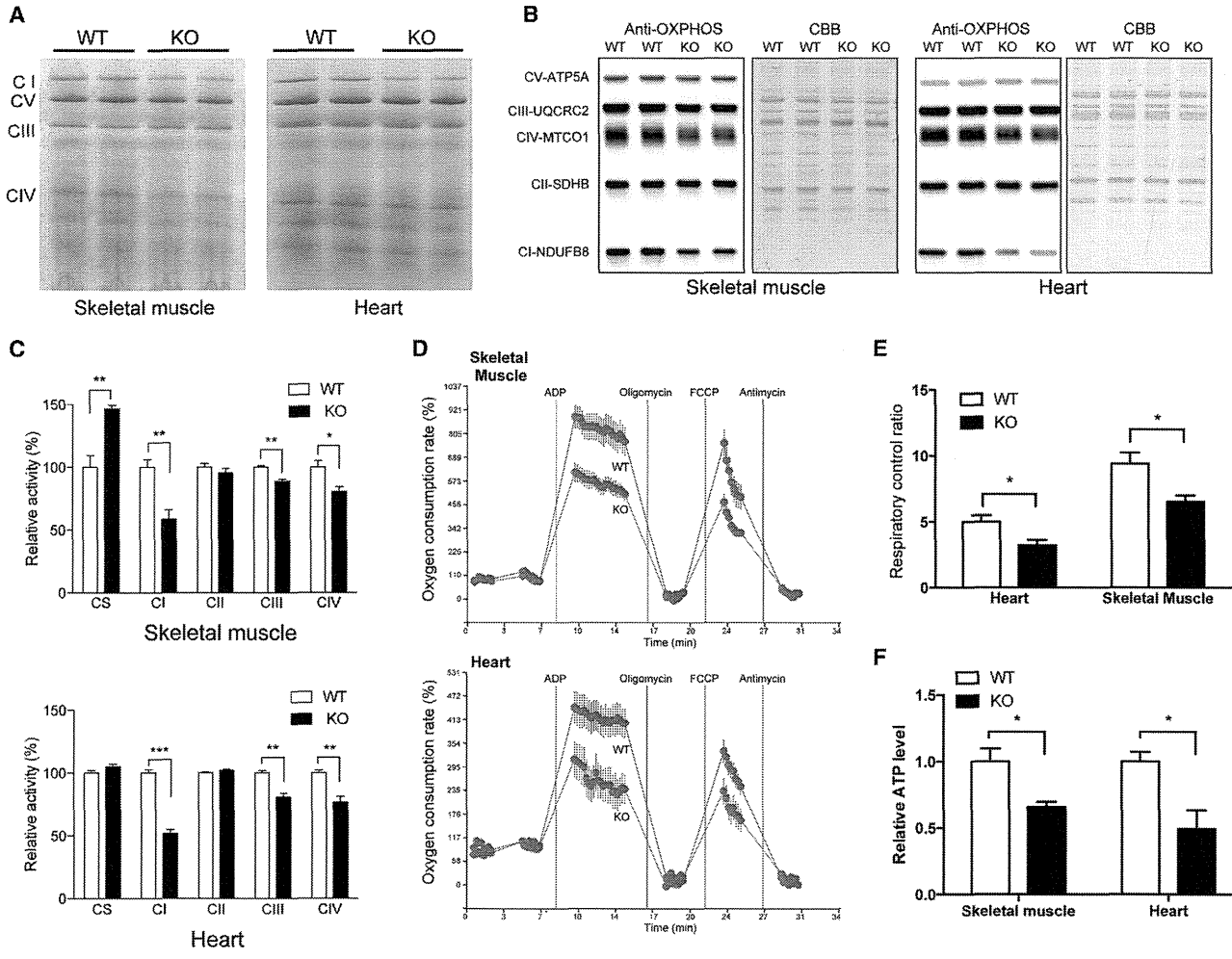

Figure 3. The Deficiency in ms^2 Modification Impaired Mitochondrial Function In Vivo

(A) Steady-state levels of complex I (CI), complex II (CIII), complex IV (CIV), and complex V (CV) in mitochondria isolated from skeletal muscle and heart tissues were examined by BN-PAGE.

(B) Steady-state levels of representative proteins of CI-CIV were examined by western blotting. CBB staining was used as loading control.

(C) The activities of CS, CI-CIV in skeletal muscle (left panel), and heart (right panel) of WT and KO mice were examined. n = 4–5.

(D and E) Respiratory coupling was decreased in Cdk5rap1-deficient mitochondria isolated from skeletal muscle and heart tissue when examined using XF24 Flux Analyzer; n = 4–5.

(F) The steady-state levels of ATP in the skeletal muscle and heart tissue of WT and KO mice were examined; n = 4 each. Data are mean ± SEM. *p < 0.05.

the mitochondrial dysfunction in KO cells, the Cdk5rap1 KO mice developed normally without obvious morphological changes in major tissues (Figures S3A and S3B). The energy expenditure and glucose metabolism in KO mice were compatible with those of WT mice (Figures S3C–S3E). Furthermore, there was no difference in neurological behaviors between KO and WT mice (Figures S3F–S3I).

Of all tissues, skeletal muscle and heart tissue are the most susceptible tissues to mitochondrial dysfunction (DiMauro and Schon, 2003). We therefore closely examined these two tissues in KO mice. Substantial decreases in the steady-state levels of complex I and IV were observed in both skeletal muscle and heart tissues of KO mice compared with WT mice, with complex I being markedly affected (Figure 3A). Accordingly, the steady-state levels of complex I and IV proteins, such as NDUFB8 and MTCO1, respectively, were markedly decreased in skeletal muscle and heart tissues of KO mice compared with WT mice (Figure 3B). As a result, complex I activity was significantly impaired in KO mice (58.6% of WT for skeletal muscle and 51.5% of WT for heart tissue) (Figure 3C). There was a mild but significant decrease in complex III and complex IV activity in KO mice (muscle: complex III, 88.8% of WT; complex IV, 80.5% of WT; heart: complex III, 80.7% of WT, complex IV, 79.8% of WT) (Figure 3C). The decrease in mitochondrial activity in the skeletal muscle of KO mice was also confirmed by cytochrome oxidase (COX) staining (Figure S3J). Accordingly, the oxygen consumption elicited by ADP and FCCP in Cdk5rap1-deficient mitochondria was significantly lower than that in WT mitochondria, indicating that electron transport and respiratory coupling were impaired in the skeletal muscle and heart tissue of KO mice (respiratory

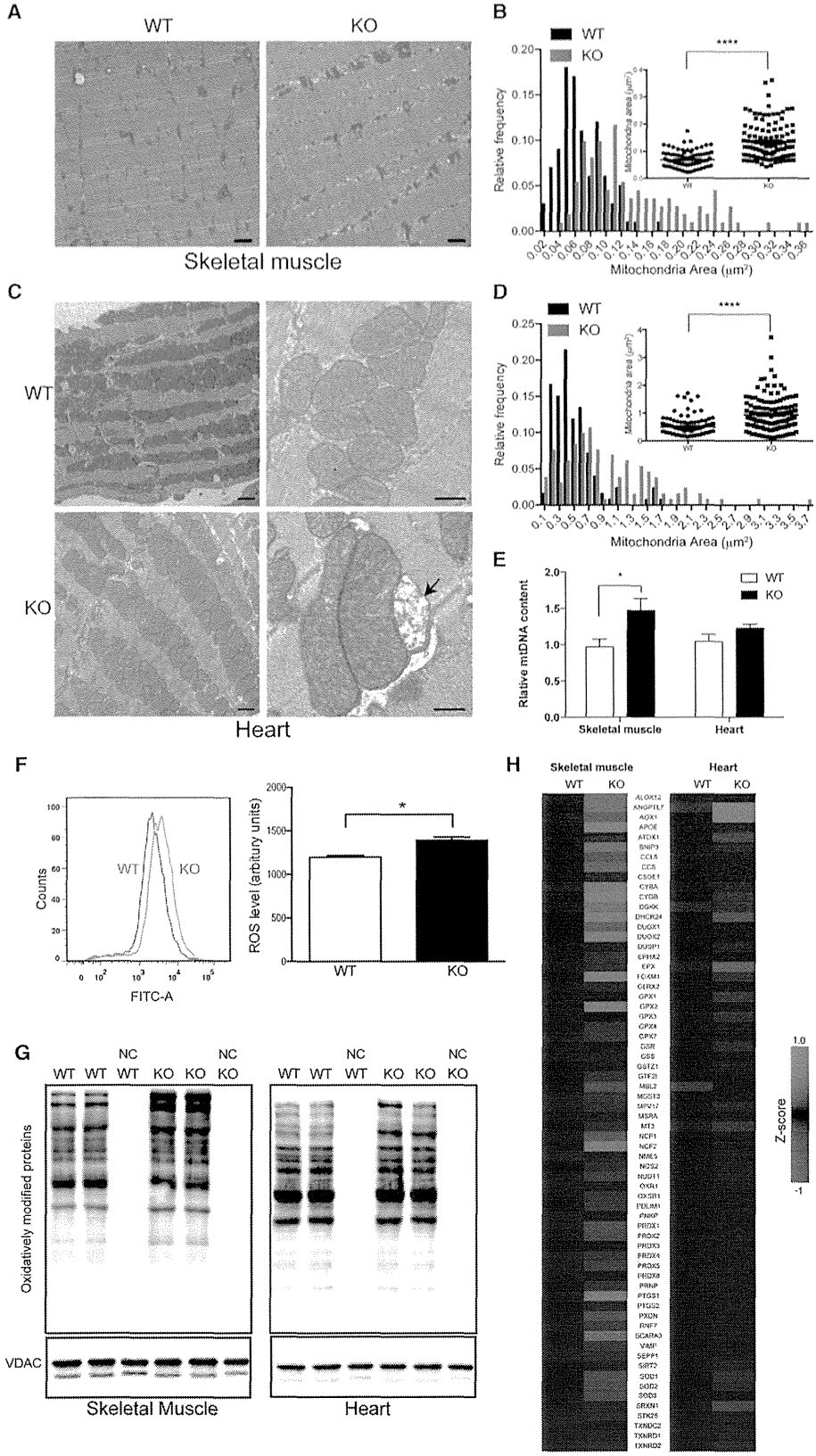

(legend on next page)

control ratio of the hearts of WT and KO: 4.9 and 3.2, skeletal muscles of WT and KO: 9.4 and 6.5, respectively; Figures 3D and 3E). Consequently, the steady-state ATP level in skeletal muscle and heart tissue of KO mice was lower than that in WT mice (Figure 3F).

Impairment of mitochondrial function usually exaggerates mitochondrial remodeling as a compensation mechanism. There was an increase in the mitochondrial mass in the skeletal muscle of KO mice as examined by electron microscopy and Gomori Trichrome staining (Figures 4A, 4B, and S3J). Strikingly, the mitochondrial was abnormally enlarged in heart tissue of KO mice (Figures 4C and 4D). A progressive disruption of cristae was occasionally observed in the mitochondria of the cardiac muscle of KO mice (arrow in Figure 4C). Furthermore, there was a significant increase in citrate synthase activity (Figure 3C) as well as relative mtDNA content (Figure 4E) in the skeletal muscle of KO mice.

Reactive oxygen species (ROS) are byproducts of mitochondrial electron transport and mainly generated from complexes I and III (Murphy, 2009). A deficiency of complexes I and III accelerates the leakage of ROS from electron transport chain and contributes to the development of mitochondrial diseases. Given the marked decrease in complex I protein level in KO mice, we investigated ROS production in KO mice (Figure 4F). The ROS level was slightly but significantly higher in KO MEF cells than that in WT MEF cells. This finding was corroborated by a moderate increase in protein carbonylation (Figure 4G) as well as oxidative stress-related gene expression in both skeletal muscle and heart tissues of KO mice (Figure 4H).

To further investigate the impact of deficiency of ms^2 modification on physiological function, we examined muscular and cardiac function in vivo. However, the treadmill performance of KO mice was comparable with that of WT mice (Figure S3K). The echocardiography examination indicated that no apparent cardiac defects were present in the KO mice (Figure S3L). Taken together, these results demonstrate that the deficiency of ms^2 modifications in mt-tRNAs impairs mitochondrial protein synthesis, which leads to a reduction of respiratory activity and increase in ROS in skeletal muscle and heart tissue. However, considering the overall phenotypes, mice seem to tolerate an up to 50% reduction of complex I activity due to the loss of ms^2 modifications under sedentary conditions.

Loss of ms^2 Modifications Accelerates OXPHOS Defects under Stressed Conditions

The mild phenotype of KO mice prompted us to challenge the mice with a ketogenic diet (KD; very high fat and ultra-low carbohydrate). Ketone bodies from KD bypass glycolysis and generate energy mostly through fatty acid oxidation in mitochondria (Laffel, 1999). Adaptation to this metabolic pressure is accompanied by mitochondrial rearrangement (Grimsrud et al., 2012). Therefore, it is conceivable that the accurate regulation of mitochondrial protein synthesis by ms^2 modification is particularly important for mitochondrial remodeling under stressed conditions.

As expected, KD treatment accelerated OXPHOS defects in the skeletal muscle and heart tissue of KO mice (Figures 4A and 4B). Complex I activity was significantly impaired in KD-fed KO mice (48.6% of the KD-fed WT for skeletal muscle and 47.7% of the KD-fed WT for heart tissue) (Figures 5A and 5B). In addition, accelerated decreases in complex III and IV activities were observed in the KD-fed KO mice (muscle: complex III, 82.9% of the KD-fed WT; complex IV, 62.9% of the KD-fed WT; heart: complex III, 75% of the KD-fed WT; complex IV, 57.8% of the KD-fed WT).

The OXPHOS defect after KD treatment exaggerated the mitochondrial remodeling pathway in both WT and KO mice. There was a ~3-fold and ~1.5-fold increase in mtDNA content in the skeletal muscle and heart tissue of both WT and KO mice fed a KD, respectively (Figure 5C). However, there was no difference in the mtDNA content in skeletal muscle and heart tissue between WT and KO mice (Figure 5C). Accordingly, subsequent electron microscopic examination revealed a marked increase in mitochondria mass (Figures 5D and 5F). In the skeletal muscles of KO mice fed a KD, mitochondrial proliferation was observed in both intermyofibrillar and subsarcolemmal mitochondria, with the latter drastically increased (Figure 5D). Importantly, KD-fed KO mice exhibited a considerable population of mitochondria with disrupted cristae in the skeletal muscle tissue (arrowheads in Figure 5D). The enlargement of mitochondria and the disruption of cristae were even more prominent in the heart tissue of KO mice fed a KD (arrows in Figure 5D). These results demonstrate that Cdk5rap1-dependent ms^2 modification is crucial for the maintenance of OXPHOS activity and mitochondrial morphology under stress.

The acceleration of the OXPHOS defect in KO mice may be due to the indirect lipotoxicity from the very high-fat diet. However, the body weight and serum metabolic profiles of KO mice fed a KD were the same as those of WT mice fed a KD (Figures S4A–S4C). There was no difference in the locomotor activity or energy expenditure between the WT and KO mice fed a KD (Figures S4D and S4E). Interestingly, the glucose level in the KD-fed KO mice was somewhat lower than that in the KD-fed WT mice (Figure S4F). Taken together, these results indicate that the progressive OXPHOS defects and mitochondrial degeneration in KD-fed KO mice directly resulted from a deficiency in Cdk5rap1-dependent ms^2 modification during mitochondrial remodeling.

Figure 4. Aberrant Mitochondrial Morphology and ROS Metabolism in KO Mice

(A–D) Mitochondria in skeletal muscle and heart tissue were examined by electron microscopy. KO mice exhibit disrupted mitochondrial morphology (A and C) and increased mitochondrial mass (B and D). Bars in (A) and the left panels of (C), 10 μm. Bars in the right panels of (C), 0.5 μm. WT, n = 100; KO, n = 112 in (B) and n = 126; KO, n = 132 in (D).

(E) The relative contents of mtDNA in muscle and heart tissue were examined; n = 6–9.

(F) ROS levels were analyzed by measuring the florescent intensity of CM-H2DCFDA in WT and MEF cells (left panel). The intensity was quantified (right panel); n = 3.

(G) Protein carbonylation levels were increased in the mitochondria of skeletal muscle and heart tissue in KO mice.

(H) Heatmap showing the differentially regulated genes involved in oxidative stress response in skeletal muscle and heart tissue of WT and KO mice; n = 4. Data are mean ± SEM. *p < 0.5, ****p < 0.0001.

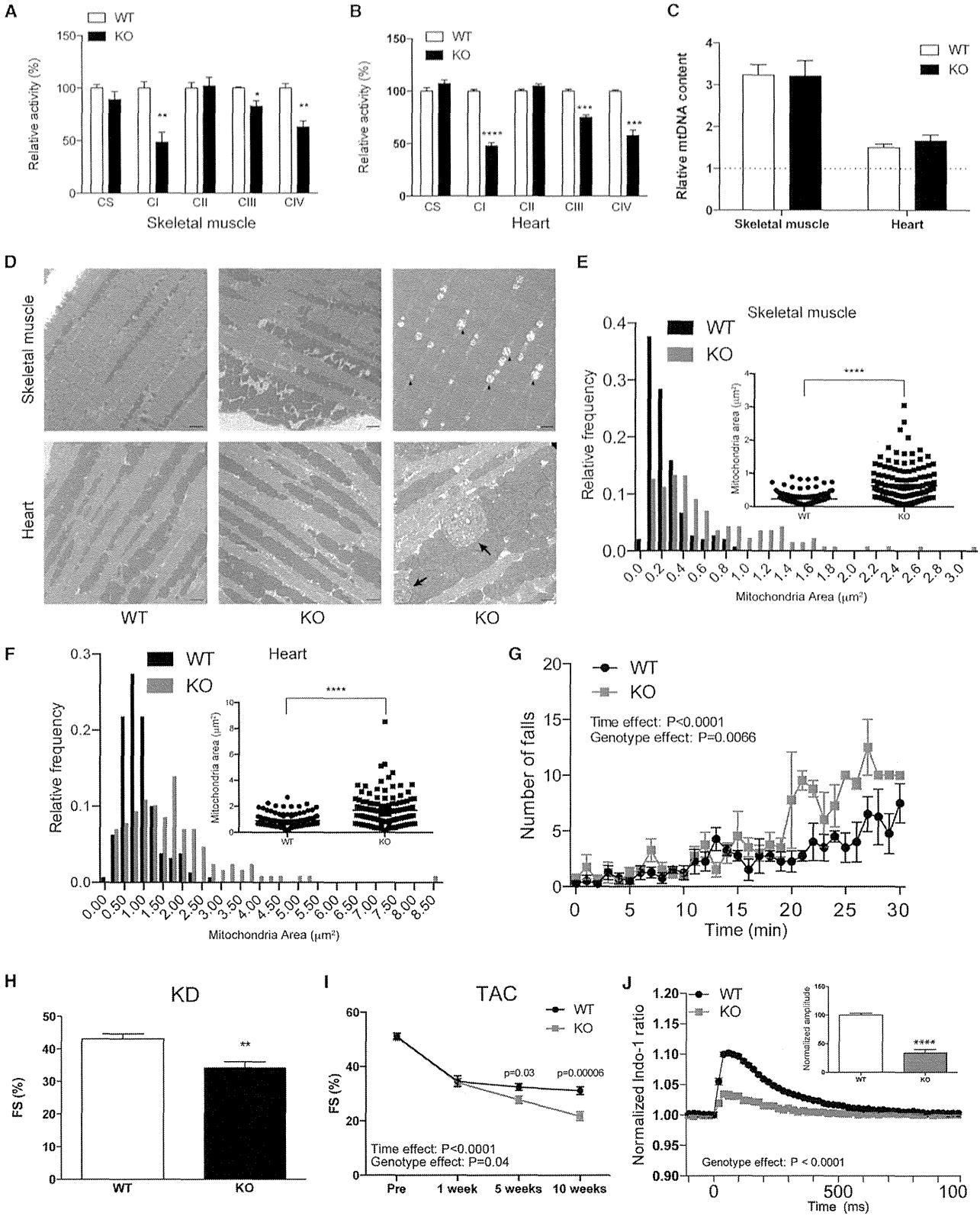

(legend on next page)

Loss of ms^2 Modification Accelerates Muscular and Cardiac Dysfunction under Stress

The KD-induced OXPHOS defect markedly accelerated the dysfunction of skeletal muscle and heart tissue in the KO mice. In a treadmill test, KO mice fed a KD showed a significant increase in the number of falls and became exhausted as early as 30 min into the test (Figure 5G). The KO mice also showed moderate cardiac hypertrophy, as indicated by an increase in heart volume, heart weight, and left ventricle posterior wall thickness (Figures S5A–S5C). The percentage of fractional shortening (FS%) in KO mice fed a KD was significantly lower than that in WT mice fed a KD (WT, 43% versus KO, 34%; Figure 5H). In addition to a KD-induced stress model, we utilized a transverse aortic constriction (TAC) model, which is a standard model for inducing cardiac dysfunction by pressure overload. Because the TAC model is also accompanied by global mitochondrial remodeling (Dai et al., 2012), we expected that a deficiency in ms^2 modification would further accelerate cardiac dysfunction. Indeed, chronic TAC resulted in a progressive cardiac hypertrophy, as indicated by an increase in heart weight and left ventricle posterior wall thickness in KO mice (WT, 7.5 mg/g body weight; KO, 11.3 mg/g body weight; Figures S5A and S5D–S5F). In WT mice, the FS% dropped from 51.2% to 34.5% 1 week after TAC but was then maintained until 10 weeks (5 weeks, 32.4; 10 weeks, 31.1; Figure 5I). In contrast, the FS% in KO mice continuously decreased after TAC and eventually decreased to as low as 21.7% (Figure 5I). Further examination in isolated cardiomyocytes revealed that the cardiac dysfunction observed in the TAC model of KO mice was associated with a decrease in calcium influx and contraction rate (Figures 5J and S5G). These results demonstrate that a deficiency of the ms^2 modifications in mt-tRNAs can cause a catastrophic defect in muscle and heart tissue under stressed conditions.

Deficiencies in ms^2 Modification Compromise the Quality of Mitochondria

Next, we investigated the molecular mechanism underlying the stress-induced acceleration of OXPHOS defects and cardiomyopathy in KO mice. Adaptation to mitochondrial stress requires coordinated protein synthesis (Dai et al., 2012). Because ms^2 modification controls decoding fidelity in a translation-rate-dependent manner, it is conceivable that a deficiency in ms^2 modification under stressed conditions might markedly compromise mitochondrial quality as well as integrity, which would result in severe OXPHOS defects and ultimately lead to myopathy and cardiac dysfunction. Indeed, a moderate increase in the complex I level was observed in WT mice treated with KD or TAC surgery (Figures 6A and 6B). In contrast, the steady-state levels of complexes I and IV levels were somewhat decreased in KD-fed and TAC KO mice when compared with NC-fed KO mice. The mitochondrial stresses increased protein carbonyltaion in both WT and KO mice. As a result, the protein carbonylation level in stressed heart tissues of KO mice was moderately higher than that in the stressed WT mice (Figure S6A). Impaired mitochondrial proteostasis exaggerates mitochondrial unfolded protein response (mt-UPR) (Durieux et al., 2011; Houtkooper et al., 2013). Accordingly, proteins involved in mtUPR, such as Yme1l1, Afg3l2, and Lonp1, were upregulated in mitochondria isolated from the hearts of KO mice treated with KD and TAC compared with WT mice (Figure 6C). Furthermore, a marked increase in polyubiquitinated proteins was observed in mitochondria isolated from the hearts of KO mice under stressed conditions (Figure 6D). Interestingly, the levels of polyubiquitination were proportional to the levels of cardiac function (FS%) in stressed KO mice (TAC > KD > NC; Figure 6D; also see Figures 5H and 5I).

Mitophagy is the hallmark of the existence of compromised mitochondria. Parkin, an E3 ubiquitin ligase, primes mitophagy by translocation to mitochondria with low membrane potentials and ubiquitination of mitochondrial proteins (Kubli and Gustafsson, 2012). Because cells with ms^2 modification deficiencies had a low basal mitochondrial membrane potential and were susceptible to stress-induced depolarization (Figures 2F and 2G), we hypothesized that mitochondrial stress might exaggerate the recruitment of Parkin to mitochondria and the acceleration of mitophagy in Cdk5rap1 KO cells. In KO cells treated with FCCP, most of the Parkin translocated to the mitochondria as soon as 2 hr after treatment, whereas similar translocation was not observed in WT cells treated with FCCP (Figure 6E; also see the separated imaged in Figure S6B). A number of large mitochondrial aggregates were surrounded by the autophagosomal membrane protein LC3 in KO cells treated with FCCP, which is indicative of acceleration of mitophagy (Figure 6F; also see the separated imaged in Figure S6C). Furthermore, we observed a number of degenerated mitochondria, with some mitochondria being degraded in autophagic vacuoles in KD-fed and TAC KO mice, by electron microscopic examination (Figure 6G). These

Figure 5. Mitochondrial Stresses Accelerated Myopathy and Cardiac Dysfunction in ms^2-Deficient Mice

(A and B) WT and KO mice at 8 weeks old were fed for KD for 10 weeks. The relative activities of CS, CI-CIV in skeletal muscle (A), and heart (B) were examined; n = 5–7 each.

(C) The relative mtDNA contents in skeletal muscle and heart tissue of KD-fed WT and KO mice were examined; n = 6–7. The dashed lines represent the relative mtDNA content in NC-fed WT mice.

(D–F) Electron microscopy examination of skeletal muscle and heart tissue show disrupted mitochondrial architecture (D) and a marked increase in mitochondrial mass (E and F) in KD-fed KO mice. Arrowheads and arrows indicate mitochondria with abnormal cristae in skeletal muscle and heart tissues of KD-fed KO mice, respectively; bars, 10 μm; WT, n = 152; KO, n = 144 in (E) and n = 161; KO, n = 130 in (F).

(G) A treadmill test performed at the end of 10 weeks of KD feeding showed that the KD induced a higher number of falls in the KO mice during acute excise compared with the WT mice; n = 5 each.

(H) The fractional shortening (FS) rate in KO mice fed with KD for 10 weeks was significantly lower than that in KO-fed WT mice; n = 10–11.

(I) WT and KO mice at 8 weeks old were subject to TAC surgery. The KO mice showed a significant decrease in FS after TAC surgery.

(J) Cardiomyocytes were isolated from WT and KO mice 10 weeks after TAC. Calcium imaging revealed a decrease in the peak calcium influx in KO cardiomyocytes. The inserted graph shows the normalized peak amplitude of calcium influx in cardiomyocytes from WT and KO mice; n = 13 for WT and n = 6 for KO. Data are the mean ± SEM. *p < 0.05. **p < 0.01, ***p < 0.001, ****p < 0.0001.

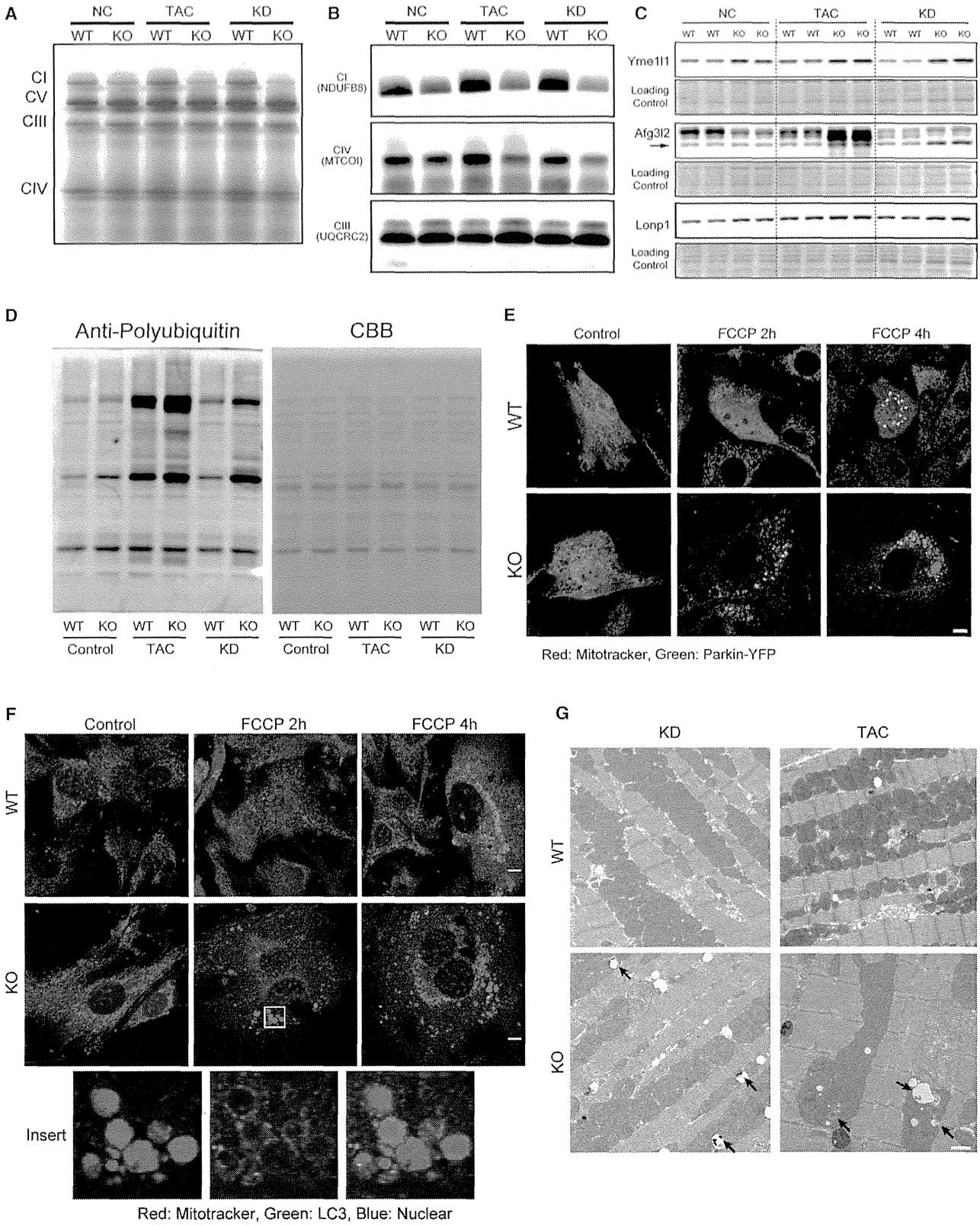

(legend on next page)

results demonstrate that stress-induced mitochondrial remodeling impaired mitochondrial protein synthesis and accelerated the decomposition of respiratory complexes, which triggered the mtUPR and mitophagy in KO mice. Thus, the accumulation of compromised mitochondria ultimately contributes to the development of myopathy and cardiac dysfunction.

Association of ms^2 Modification with Mitochondrial Disease

Because the pathological phenotypes of KO mice resembled those of mitochondrial disease, we speculated that ms^2 modification might be involved in mitochondrial disease. We investigated the ms^2 modification level in peripheral blood cells collected from MELAS patients who carry the A3243G mutation (Figure S7A). Because of the limited number of clinical RNA samples, we adapted the quantitative PCR-based method (Xie et al., 2013), which was originally developed to examine the ms^2 level of ms^2t^6A in cytosolic $tRNA^{Lys(UUU)}$, to sensitively examine the ms^2 modification level ms^2i^6A in mt-tRNAs (Figures S7B–S7E). Strikingly, the heteroplasmy level of mutant mt-DNA was significantly correlated with the ms^2 modification levels of four mt-tRNAs, but not with the cytosolic tRNALys(UUU) (Figures 7A–7D and S7F). Interestingly, the mutant mtDNA level was not correlated with the expression level of *CDK5RAP1*, suggesting that the decrease in ms^2 modifications was not due to a deficiency in Cdk5rap1 (Figures S5D–S5G). Because the A3243G mutation is located in the mtDNA region corresponding to $mt\text{-}tRNA^{Leu(UUR)}$, the decrease in the ms^2 levels of $tRNA^{Trp}$, $tRNA^{Phe}$, $tRNA^{Tyr}$, and $tRNA^{Ser(UCN)}$ was likely not caused by the A3243G mutation but, rather, was due to secondary effects. Cells bearing A3243G mutations in mtDNA exhibit a marked reduction of mitochondrial protein synthesis and an increase in the oxidative stress level (Crimi et al., 2005; Ishikawa et al., 2005). Because Cdk5rap1 contains highly oxidation-sensitive [4Fe-4S] clusters (Arragain et al., 2010), we speculated that the excess oxidative stress originated from mutant mitochondria might result in a collateral inhibition of Cdk5rap1 activity. Indeed, cells treated with sublethal doses of H_2O_2 showed a rapid decrease in ms^2 modification, which was completely reversed by adding 10 mM pyruvate, which serves as an antioxidant (Figures 7E–7G). In addition, treatment of cells with an NO donor such as SNAP and NOC18 significantly reduced the ms^2 modification level, which was reversed by the addition of the NO scavenger PTIO (Figure 7H). Taken together, these results suggest that oxidative stress-induced decreases in ms^2 modifications might compromise the quality of the mitochondria and contribute to the progression of mitochondrial disease.

DISCUSSION

Regulation of Mitochondrial Protein Synthesis by Cdk5rap1-Mediated ms^2 Modification

In the present study, we revealed the important physiological functions of ancient mitochondrial ms^2 modifications in mice and human. Using Cdk5rap1 KO mice, we provide direct evidence that Cdk5rap1 catalyzes the ms^2 modifications of $mt\text{-}tRNA^{Phe}$, $mt\text{-}tRNA^{Trp}$, $mt\text{-}tRNA^{Tyr}$, and $mt\text{-}tRNA^{Ser(UCN)}$ in mammalian cells. The ms^2 group at the A37 of tRNA can directly participate in crossstrand stacking with the first nucleotide of the codon of the mRNA to maintain the reading frame (Jenner et al., 2010). Indeed, a deficiency in the ms^2 modification of ms^2i^6A impaired reading frame maintenance in bacteria and caused defective mitochondrial protein synthesis in Cdk5rap1 KO mice. Interestingly, nuclear-encoded mitochondrial protein, such as NDUFB8 in complex I, was also decreased in KO mice. The indirect decrease of NDUFB8 is most likely due to the poorly assembled respiratory complexes in KO mice. A previous study has shown that a deficiency in a single subunit in complex I could compromise complex formation and cause the proteolysis of other subunits (Karamanlidis et al., 2013). Our results thus demonstrate that the ms^2 modification of mt-tRNAs is indispensable for mitochondrial protein synthesis and the proper assembly of respiratory complexes.

Whereas only one transcript of *Cdk5rap1* has been found in mice, multiple splicing variants of human *CDK5RAP1* are listed in the database (Figure S1A). One transcript of human *CDK5RAP1* encodes a short form of CDK5RAP1 without a mitochondrial localization signal (Q95SZ6-2 in Figure S1A), which raises the possibility that CDK5RAP1 might regulate cellular function by modifying cytosol RNAs (Reiter et al., 2012). However, there was no detectable ms^2i^6A in total RNA isolated from KO MEF cells expressing the cytosolic form of Cdk5rap1 with the enzyme activity preserved. These results clearly suggest that Cdk5rap1 does not modify nuclear DNA-derived RNAs in murine cells. Furthermore, the defective mitochondrial protein synthesis observed in Cdk5rap1 KO mice may be directly caused by the loss of ms^2 modifications in mt-tRNAs.

Deficiency of ms^2 Modification and Its Physiological Outcome

This study revealed unique phenotypic outcomes of Cdk5rap1 KO mice in response to distinct environmental conditions. Under sedentary conditions, the skeletal and cardiac functions of the

Figure 6. The Deficiency in ms^2 Modification Compromises Mitochondrial Protein Quality under Stressed Conditions

(A) Steady-state levels of CI, CIII, CIV, and CV in heart tissue in WT and KO mice treated with NC, KD, and TAC surgery were examined by BN-PAGE.

(B) The steady-state levels of CI protein NDUFB8, CIV protein MTCOI, and CIII protein UQCRC2 in heart tissue in WT and KO mice treated with NC, KD, and TAC surgery were examined by BN-PAGE followed by western blotting. UQCRC2 was used as a loading control.

(C) The protein levels of Yme1l1, Afg 3l2, and Lonp1 were examined in heart tissues from WT and KO mice treated with NC, KD, and TAC surgery. Membranes stained with CBB were used as a loading control.

(D) Enhanced polyubiquitination was observed in the mitochondria in the hearts of KO mice under each stress.

(E) WT and KO cells transfected with Parkin-YFP were treated with 10 μM FCCP for 2 and 4 hr; bar, 10 μm.

(F) WT and KO cells were treated with 10 μM FCCP for 2 and 4 hr. The cells were then stained with an anti-LC3 antibody and Mitotracker. The inserted box shows mitochondria surrounded by the LC3 protein and is magnified in the bottom panels; bar, 10 μm.

(G) Electron microscopy of mitochondria in heart tissue from WT and KO mice treated with KD or TAC surgery. Arrows indicate the autophagic vacuoles; bar, 10 μm.

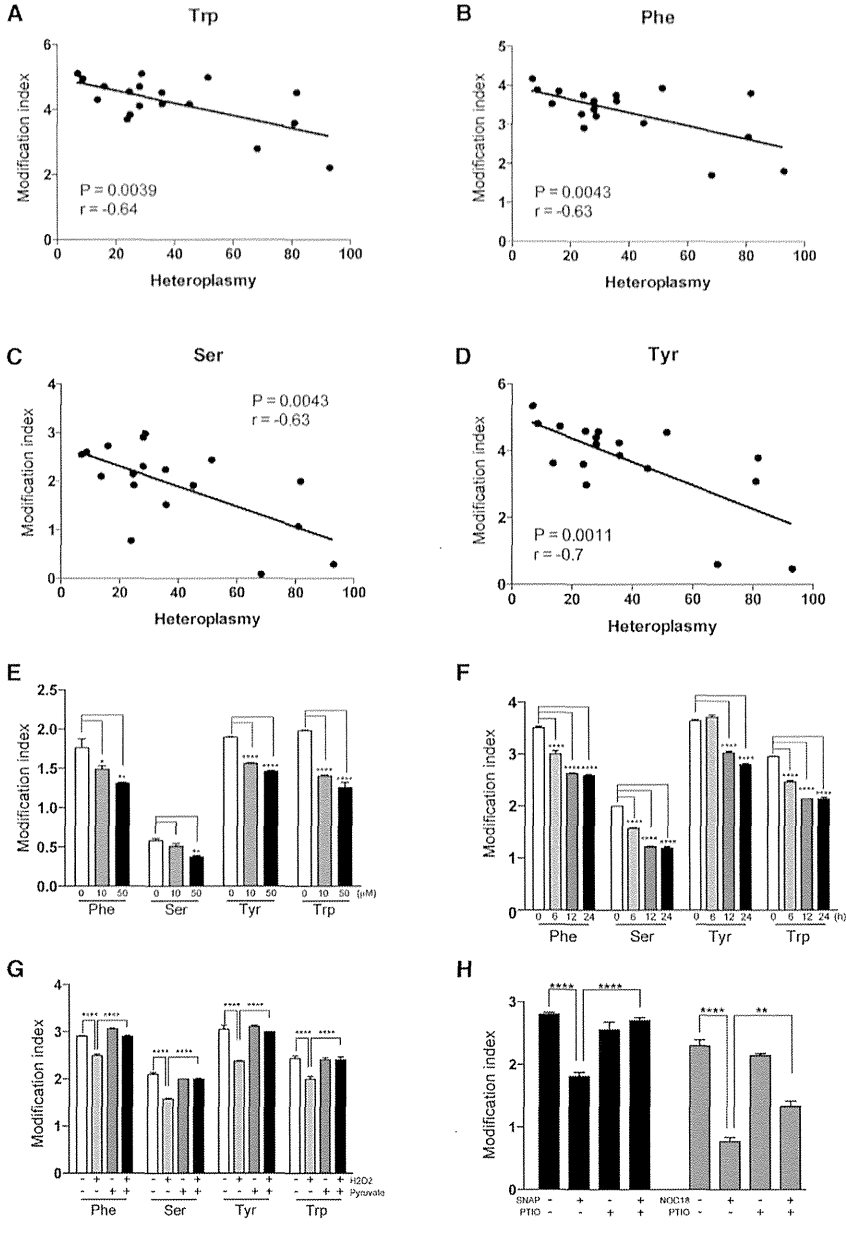

Figure 7. Association of ms^2 Modifications with MELAS

(A–D) Negative correlation of the ms^2 modification level of mt-$tRNA^{Trp}$ (A), mt-$tRNA^{Phe}$ (B), mt-$tRNA^{Ser(UCN)}$ (C), or mt-$tRNA^{Tyr}$ (D) with the heteroplasmy level in MELAS patients; n = 18 each.

(E) Treatment with H_2O_2 reduced the level of ms^2 modification of mt-tRNAs in HeLa cells. Cells were treated with 10 μM or 50 μM H_2O_2 for 24 hr, and the ms^2 modification levels were examined by qPCR; n = 4 each.

(F) Time-dependent decreases in ms^2 modification after H_2O_2 treatment in HeLa cells. Cells were treated with 50 μM H_2O_2 for 6, 12, and 24 hr; n = 4 each.

(G) HeLa cells were treated with 50 μM H_2O_2 for 24 hr in the presence or absence of 10 mM pyruvate. The decrease in the ms^2 modification level was prevented by pyruvate; n = 4 each.

(H) HeLa cells were treated with NO donors, 100 μM SNAP or 100 μM NOC18 for 24 hr in the presence or absence of PTIO. The ms^2 modification level of mt-$tRNA^{Trp}$ was examined by qPCR; n = 4 each. Data are the mean ± SEM. *p < 0.05. **p < 0.01, ****p < 0.0001.

Cdk5rap1 KO mice were compatible with those of the WT mice, despite the marked decrease in respiratory activities and regardless of the increase of oxidative stress. The mitochondrial dysfunction in KO mice might be compensated by the remodeling of mitonuclear protein balance, which serves as a protective mechanism by inducing mtUPR (Houtkooper et al., 2013). Indeed, in contrast to the decrease of mitochondrial protein synthesis, several cytosolic proteins appear to be upregulated in KO cells (right panels in Figure 2A). This mitonuclear protein imbalance might contribute to the upregulation of basal mtUPR in muscle and heart tissues of KO mice (Figure 6C). Furthermore, a collective increase of ROS metabolism genes, including ROS scavenger genes such as *ApoE*, *DHCR24*, and *SRXN1*, might ameliorate oxidative stress and protect the muscular and cardiac functions in KO mice. Similar to our results, previous studies have found no adverse phenotypes under basal conditions in transgenic mice with respiratory defects (Karamanlidis et al., 2013; Wenz et al., 2009). Our results thus support the current perspective that mitochondrial dysfunction, depending on its degree, may not immediately produce a pathological phenotype under sedentary conditions.

In contrast, under stressed conditions, Cdkrap1 KO mice exhibited apparent skeletal muscle and heart dysfunctions. The defective mitochondrial protein synthesis caused a marked decrease in protein levels and activities of complexes I and IV in KO mice under stressed conditions. The progressive disruption of respiratory complexes, which exaggerates mtUPR and mitophagy, thus largely compromised mitochondria quality and led to myopathy in KO mice. Recent studies have shown that Parkin-mediated mitophagy is critical for the removal of damaged mitochondria and thus protects cardiac function under stressed conditions (Hoshino et al., 2013; Chen and Dorn, 2013). However, given the observation of a number of degenerated mitochondria in KO mice (Figures 4D and 5G), the extent of mitochondria damage in KO mice was likely beyond the maintenance capacity of mitophagy, which ultimately led to catastrophic mitochondrial dysfunction and myopathy. In addition, the acceleration of complex I defect was associated with a modest increase of oxidative stress, which could trigger mtUPR and cause cytotoxicity in stressed KO mice (Runkel et al., 2013). However, compared with the progressive impairment of mitochondria quality, the degree of increase of ROS after mitochondrial stress was rather small in